Chromatin Affinity Purification and Quantitative Mass Spectrometry Defining the Interactome of Histone Modification Patterns*⑤

Miroslav Nikolov‡, Alexandra Stützer§, Kerstin Mosch§, Andrius Krasauskas¶, Szabolcs Soeroes§, Holger Stark¶, Henning Urlaub‡‖, and Wolfgang Fischle§****

DNA and histone modifications direct the functional state of chromatin and thereby the readout of the genome. Candidate approaches and histone peptide affinity purification experiments have identified several proteins that bind to chromatin marks. However, the complement of factors that is recruited by individual and combinations of DNA and histone modifications has not yet been defined. Here, we present a strategy based on recombinant, uniformly modified chromatin templates used in affinity purification experiments in conjunction with SILAC-based quantitative mass spectrometry for this purpose. On the prototypic H3K4me3 and H3K9me3 histone modification marks we compare our method with a histone N-terminal peptide affinity purification approach. Our analysis shows that only some factors associate with both, chromatin and peptide matrices but that a surprisingly large number of proteins differ in their association with these templates. Global analysis of the proteins identified implies specific domains mediating recruitment to the chromatin marks. Our proof-of-principle studies show that chromatin templates with defined modification patterns can be used to decipher how the histone code is read and translated. *Molecular & Cellular Proteomics* 10: 10.1074/mcp.M110.005371, 1–16, 2011.

DNA methylation and histone post-translational modifications (PTM)[1] play important roles in regulating chromatin states and thereby the use and readout of the genome. Trimethylation of lyinse 4 (H3K4me3) and lysine 9 (H3K9me3) of histone H3 have, for example, been connected to transcriptional activation and repression, respectively. They therefore present a prototypic pair of antagonistic histone PTMs.

Generally, chromatin marks either influence chromatin packaging directly or via recruitment of specific proteins and multiprotein complexes that mediate downstream effects (1, 2). Candidate approaches of individual factors or using targeted libraries of protein families together with histone tail peptide affinity purification experiments carried out in isolation or on peptide arrays have identified a number of proteins that specifically interact with individual chromatin marks (see for example ref. 3–6). These include factors containing methyl-DNA binding domains as well as chromodomains, plant homeodomain (PHD) fingers, tudor domains, and ankyrin repeats interacting with histone methyl-lysine residues. Further, 14-3-3 proteins interacting with histone phospho-serine residues and bromodomain containing factors binding to histone acetyl-lysine residues have been described (7). *In vitro* studies have characterized the exact binding specificities of several proteins containing these domains. Also, structural insights are now available for a number of chromatin mark binding complexes (7, 8).

Interestingly, the interactions of individual domains of chromatin modification binding proteins with their cognate marks

[1] The abbreviations used are: PTM, post translational modification; SILAC, stable isotope labeling by amino acids in cell culture; H3K4me3, histone H3 lysine 4 trimethylation; H3K9me3, histone H3 lysine 9 trimethylation; PHD, plant homeodomain; MudPIT, multidimensional protein identification technology; TAF, TATA box binding protein (TBP)-associated factor; PHF8, PHD finger protein 8; CHD1, chromodomain-helicase-DNA-binding protein 1; ING2, inhibitor of growth family member 2; WDR5, WD repeat domain 5; HP1, heterochromatin protein 1; CBX, chromobox homolog; UHRF1, ubiquitin-like with PHD and ring finger domains 1; CDYL, chromodomain protein Y-like; MPHOSP8, M-phase phosphoprotein 8; SPIN1, spindling 1; FANCF, Fanconi anemia, complementation group F; ADNP, activity-dependent neuroprotector homeobox; ZMYM3, zinc finger MYM-type 3; ACTL8, actin-like 8; SMCHD1, structural maintenance of chromosomes flexible hinge domain containing 1; TFIID, TATA binding protein; POGZ, pogo transposable element with ZnF domain; ZnF, zinc finger; DAXX, death-domain associated protein; DNMT1, DNA (cytosine-5-)-methyltransferase 1; H3K27me3, histone H3 lysine 27 trimethylation; SRA, SET and RING associated; HAT, histone acetyl transferase; SNF2, sucrose non fermentable 2; ARID, AT-rich interaction domain; Myb, myeloblastosis oncogene like; SANT, switching-defective protein 3 (Swi3) adaptor 2 (Ada2) nuclear receptor co-repressor (N-CoR) transcription factor (TF)IIIB; H4K20me3, histone H4 lysine 20 trimethylation; H3K27me1, histone H3 lysine 27 monomethylation; H3R2me2, histone H3 arginine 2 dimethylation; H4R3me2, histone H4 arginine 3 dimethylation.

are rather weak (interaction strength in the micromolar range) (9). Although the study of interactions of individual proteins with DNA methylation or distinct histone PTM marks has been central to our current understanding of chromatin mediated processes, it is emerging that patterns of marks rather than individual modifications direct functional states of chromatin (10, 11). Here, factors containing multiple domains interacting with different chromatin marks have gained high interest (12). Multivalent binding might not only allow for stronger and thereby more discriminatory interaction than single domain binding, but could also direct readout of complex patterns of modifications. Also, multiprotein complexes appear to contain several factors with the same or distinct chromatin mark recognition functionality thereby possibly establishing more stable interaction.

Gaining global insight into the relationship of chromatin modifications and functional states of chromatin ultimately requires isolation and characterization of intact chromatin domains from cells. In absence of such experimental systems *in vitro* approaches that mimic and incorporate different DNA methylation and histone PTM configurations will likely be extremely useful in defining the complement of factors that targets a given pattern of chromatin marks. Here, DNA and/or histone tail peptide affinity purification experiments can only be of limited value as only individual or shortly spaced combinatorial patterns of modifications can be analyzed (see for example ref. 13).

Nonquantitative mass spectrometry (*e.g.* MudPIT, ref. 14) analysis of differential affinity purification reactions has been useful in identifying proteins binding a given target (4). However, because these methods do not provide sufficient quantitative information on the proteins recovered in separate experiments in the first place, factors that bind two separate matrices (*e.g.* sample and control) with different strength will not be necessarily recognized as specific interaction partners of either one. Therefore, different mass spectrometry methods have been introduced that allow identification and sensitive quantification of proteins in matched experiments (15). Especially, isotope labeling by amino acids in cell culture (SILAC) has proven useful in various proteomics based approaches (16). Here, we set out to establish an *in vitro* system usable for the analysis of complex chromatin modification patterns based on recombinant, uniformly modified chromatin templates in combination with quantitative SILAC-based mass spectrometry analysis. In this manner, we defined the interactome of the H3K4me3 and H3K9me3 chromatin marks. Surprisingly, only some factors were also recruited to corresponding histone N-terminal peptides in parallel experiments. Our results set the stage for using chromatin-based affinity approaches to investigate how the histone code is read and translated on a global scale.

EXPERIMENTAL PROCEDURES

Cell Culture, Labeling, and Nuclear Extract Preparation—HeLa S3 cells were grown in lysine- and arginine-deficient Dulbecco's modified Eagle's medium supplemented with 10% dialyzed fetal bovine serum (PAA, Pasching, Austria). One cell population was supplemented with normal isotope containing L-lysine and L-arginine (Sigma, Munich, Germany) and another with heavy isotope labeled $^{13}C_6$-lysine and $^{13}C_6^{15}N_4$-arginine (Euriso-Top, Saint-Aubin Cedex, France) generating mass shifts of +6 and +10 Da, respectively. Cells were grown for at least six passages at smaller volumes and then expanded to 2 l in spinner flasks ($0.5–1.0 \times 10^6$ cells/ml) (16). The cells were then transferred to a 5 l fermenter (Applikon, Schiedam, Netherlands) and grown under standard conditions ($2.5–5.0 \times 10^6$ cells/ml). Harvested cells were used to prepare nuclear extract according to standard procedures (17).

Peptides—Peptides containing the 20 N-terminal amino acids of histone H3 were synthesized in unmodified and modified form using Fmoc (N-(9-fluorenyl)methoxycarbonyl)-based solid-phase synthesis H3unmodified: ARTKQTARKSTGGKAPRKQL; H3K4me3: ARTK(me3)-QTARKSTGGKAPRKQL; H3K9me3: ARTKQTARK(me3)STGGKA-PRKQL. Peptides contained a C-terminal non-native lysine biotinylated at the ε-amino group for affinity purification reactions or were transformed to thioacetamidthiophenylesters for native protein ligation (18–20).

Native Protein Ligation—Histone modifications were achieved by native protein ligation using histone H3 (1–20) thioester peptides and recombinant *X. laevis* histone H3Δ1–20,A21C as described (21). Reactions were carried out in 100 mM potassium phosphate (pH 7.9), 3 M guanidine-HCl, 0.5% v/v benzyl mercaptan, 0.5% v/v thiophenol at 25 °C with vigorous mixing. Crude reaction mixture was diluted 50-fold into SAU-200 buffer (7 M deionized urea, 20 mM sodium acetate (pH 5.2), 1 mM EDTA, 1 mM dithiothreitol, 200 mM NaCl), applied to a 5 ml Hi-Trap SP-Sepharose high performance cation exchange column (GE Healthcare, Munich, Germany), and eluted with a linear NaCl gradient from 200 to 600 mM in 10 column volumes. Protein was dialyzed extensively against 2 mM dithiothreitol at 4 °C, lyophilized and stored at −80 °C. Routinely we set up ligation reactions containing 27 mg histone (2 μmol), 23 mg thioacetamidthiophenylester histone H3 peptide (10 μmol) in 10 ml reaction volume. After purification on average 10 mg ligated histone H3 was obtained (0.6 μmol). Purity and identity of thioester peptides and ligated proteins was confirmed by analytical high-performance liquid chromatography, mass spectrometry, and SDS-PAGE (see supplemental Fig. S1).

Recombinant Chromatin—Recombinant chromatin was prepared essentially as described (22). Briefly, recombinant wild type *Xenopus laevis* histones were expressed in *Escherichia coli* and purified as described (23). Assembly of histone octamers containing modified and unmodified histone H3 as well as nucleosome array reconstitution was performed by salt dialysis on biotinylated 12 × 200 × 601 DNA template as described (23, 24). Quality of chromatin reconstitution was monitored by native agarose gel electrophoresis, MNase digest, and analytical ultracentrifugation (see supplemental Fig. S2).

Peptide and Chromatin Affinity Purifications—Affinity purifications were performed essentially as described using two separate preparations of nuclear extract (22). Each experiment was performed in "forward" (light extract, unmodified chromatin and peptide; heavy extract, modified chromatin and peptide) and "reverse" (light extract, modified chromatin and peptide; heavy extract, unmodified chromatin and peptide) label swap affinity purification. For peptide affinity purifications, 40 μl prewashed streptavidin coated paramagnetic beads (Pierce, Rockford, IL) were saturated with 10 μg biotinylated histone peptide overnight at 4 °C. A 0.5 ml aliquot of precleared HeLa S3 nuclear extract (light or heavy isotope labeled) was incubated with the peptide-bound paramagnetic beads for 4 h while rotating. Beads

were washed three times with 1 ml of PD150 buffer (20 mM HEPES pH 7.9, 150 mM NaCl, 0.1% Triton X-100, 5% glycerol). Beads from parallel affinity purification reactions using unmodified and modified peptides were mixed (25) and bound proteins were eluted with LDS sample buffer (Invitrogen, Carlsbad, CA). Chromatin affinity purifications were performed accordingly using 50 μg chromatin and 200 μl paramagnetic beads. To improve SDS-PAGE resolution, eluates of chromatin affinity purification reactions were incubated with 1 kU benzonase (Calbiochem, San Diego, CA) nuclease for 1 h at 37 °C.

Western Blotting—Primary antibodies used were: αH3K4me3 (1: 2,000, Abcam, Cambridge, UK), αH3K9me3 (1:1,000, Millipore, Billerica, MA), αFLAG (1:1,000, Sigma, Munich, Germany), and αSMCHD1 (1:1,000, Abcam, Cambridge, UK).

LC-MS/MS—Eluted proteins were separated on 4–12% gradient SDS-PAGE gels (Invitrogen, Carlsbad, CA) and stained with Colloidal Coomassie Blue. Each gel lane was cut into 23 equal gel slices and proteins therein were in-gel digested with trypsin (Promega, Madison, WI) as described (26). Tryptic peptides from each gel slice were extracted and analyzed by nanoflow HPLC (Agilent, Boeblingen, Germany) coupled to nanoelectrospray LTQ-Orbitrap XL mass spectrometer (Thermo Fisher Scientific, Waltham, MA) operating in positive ion mode. Peptides were first loaded and desalted onto an in-line trap column (1.5 cm length, 150 μm inner diameter, packed in-house with Reprosil AQ-5 μm/300Å) and then separated on analytical column (15 cm length, 75 μm inner diameter, as trap column) at flow-rate 250 nL/min and linear gradient from 7.5 to 37.5% acetonitrile in 0.1% (v/v) formic acid for 50 min. Data-dependent acquisition of eluting peptides was applied and consisted of one survey scan in Orbitrap (with resolution set to 30,000 at m/z 400 and automatic gain control target at 10^6) followed by MS/MS of the five most intense precursors in the LTQ using collision-induced decay fragmentation with previously fragmented ions dynamically excluded for 90 s. Each sample was analyzed in three technical replicates.

Data Analysis—Raw MS files from LTQ-Orbitrap XL were analyzed by MaxQuant software (version 1.0.13.13) (27). Peak lists generated by Quant.exe (the first module of MaxQuant) were searched by Mascot search engine (Mascot Daemon 2.2.2; Matrix Science, London, UK) using International Protein Index (IPI) Human protein database (version 3.73, June 2010, containing 89739 entries) supplemented with 179 common contaminants (*e.g.* keratins, serum albumin) and concatenated with the reverse sequences of all entries. Mascot search parameters were used as follows: Carbamidomethylation of cystein and oxidation of methionine were set as variable modifications, tryptic specificity with no proline restriction and up to two missed cleavages was used. The initial mass tolerance used was 7 ppm and for MS/MS 0.6 Da. Only peptides with minimal length of six amino acids were considered. Peptides were filtered for maximum false discovery rate of 1% in MaxQuant. Only unique and razor peptides with posterior error probability of less than 0.05 and proteins with ratio count of at least three were accepted and used for quantification (27). Results from MaxQuant were analyzed and visualized with R (script details are available in supplemental Experimental Procedures). Proteins showing opposite ratios between forward and reverse label-swap experiments were manually validated using MaxQuant Viewer, marked as potential false positives and included into a separate list that was not used for plotting with R. All proteins are listed in supplemental Tables S1–S4 with accession numbers, number of unique peptides, % sequence coverage, quantification significance, and variability, as reported by MaxQuant.

For enrichment analysis-based hierarchical clustering, the quantified proteins from each experiment were divided into five lists corresponding to enrichment ratio cutoffs of below −4 to −4, −4 to −2, −2 to 2, 2 to 4, and above 4. Proteins from each list were searched for enriched protein domains terms using DAVID (28) without enrichment score cutoff (databases used: UniProt, Sequence Feature, InterPro, PIR Superfamily, PFAM, SMART). The resulting lists were then collated using a Python script (script details are available in supplemental Experimental Procedures; http://www.python.org). All terms being enriched with EASE score from DAVID of better than 0.1 in at least one of the lists were included into a combined list. Hierarchical clustering was done in the R statistical environment using the Euclidean distance function and combined linkage method.

Plasmids—cDNAs encoding mACTL8 (IMAGE ID:IRATp970D1240D), mFANCF (IMAGE ID:IRATp970B10123D), mSPIN1 (IMAGE ID: IRAVp968H0931D), and mADNP (FANTOM3 ID:6330563C07) were obtained from Imagenes. cDNA encoding mZmym3 was amplified from cDNA isolated from NIH3T3 cells (reference sequence GenBank NM_019831.3). cDNAs were cloned into a modified pcDNA3.1 vector fusing the 3′ end to a 2xHA-2XFLAG tag. The following primer pairs were used for PCR amplification. pCDNA-Actl8-HAHAFlFl(BamHI - NotI), fwd: GAGCTCGGATCCATGGCTTCAAGAACCGTTATC, rev: GGGTATGCGGCCGCCATCCTCATATGCTCACCATAC; pCDNA-FancF-HAHAFlFl (BamHI - NotI) fwd: GAGCTCGGATCCATGGAATC-CCTTCTGCAGCAC, rev: GGGTATGCGGCCGCTACAGAACTGAG-GCCTGCGC; pCDNA-SPIN1-HAHAFlFl(AflII - NotI) fwd: TTTAAACT-TAAGCTTATGAAGACCCCATTCGGGAAG, rev: GGGTATGCGG-CCGCGGATGTTTTCACCAAATCGTAG; pCDNA-Zmym3-HAHAFlFl-(AflII - NotI) fwd: TTTAAACTTAAGATGGACCCCAGTGATTTCCC, rev: GGGTATGCGGCCGCGTCTAGGTCTTCTTCCCCAG; pCDNA-ADNP-HAHAFlFl(BamHI - NotI) fwd: GAATTGGGATCCATGTTCCAACTTC-CTGTCAAC, rev: GGGTATGCGGCCGCGGCTTGCTGGCTGCT-CAGC. Details of cloning are available upon request.

Cell Culture and Transfection—NIH3T3 and HEK 293T (ATCC) cells were grown at 37 °C in a humidified atmosphere, 5% CO_2 using Dulbecco's modified Eagle's medium supplemented with 10% fetal bovine serum, 2 mM glutamine, and 1 × penicillin/streptomycin (Invitrogen, Carlsbad, CA). Transfection was performed using JetPEI reagent (Biomol, Hamburg, Germany). Typically 6 μl JetPEI reagent and 3 μg of plasmid were used per coverslip in a 6-well plate (NIH3T3) and 40 μl JetPEI reagent and 20 μg of plasmid were used per 15 cm dish (HEK 293T).

Immunofluorescence—Cells were seeded on glass cover slips in 6-well plates. Cover slips were washed two times with phosphate-buffered saline (PBS) and fixed for 10 min in 3% paraformaldehyde in PBS at 37 °C. Cover slips were washed once with PBS and cells were permeabilized for 10 min (0.5% Triton X-100 in PBS). Cells were washed once with 0.2% Triton X-100 in PBS before blocking for 30 min in blocking solution (1 × PBS, 2% BSA, 0.2% Triton X-100 (v/v), 5% normal goat serum (v/v)). Primary antibodies (anti-FLAG M2 (Sigma, Munich, Germany) 1:1,000; anti-H3K9me3; anti-H3K4me3 (both 1:500, Millipore, Billerica, MA)) and fluorescently labeled secondary antibodies (anti-mouse-Alexa555 and anti-rabbit-Alexa488 (Molecular Probes, Eugene, OR) 1:1,000) were applied in blocking solution for 1 h at room temperature. Cover slips were washed two times with 0.2% Triton X-100 in PBS and five times in water. Cover slips were mounted in Mowiol including 50 μg/ml DAPI. Slides were dried overnight at RT and analyzed using a Leica TCS SP5 confocal microscope.

RESULTS AND DISCUSSION

Experimental Set-up—To obtain homogenously modified histone H3 proteins containing H3K4me3 or H3K9me3 we used native protein ligation of synthetic histone H3 (1–20) N-terminal peptides containing these marks and core recombinant histone H3Δ1–20,A21C protein expressed in bacteria (Fig. 1A, supplemental Fig. S1) (21). In conjunction with other core histones H2A, H2B, and H4 octamers were assembled

FIG. 1. **Set-up and workflow of the peptide and chromatin affinity purification system.** A, Scheme of reconstitution of recombinant, uniformly modified chromatin using native protein ligation. B, The indicated chromatin templates were analyzed before and after affinity purification reactions using SILAC-labeled nuclear HeLa S3 extract by Western blot using the specified antibodies. Ponceau staining of the membrane served as loading control. C, Workflow of the chromatin affinity purification experiment and its analysis.
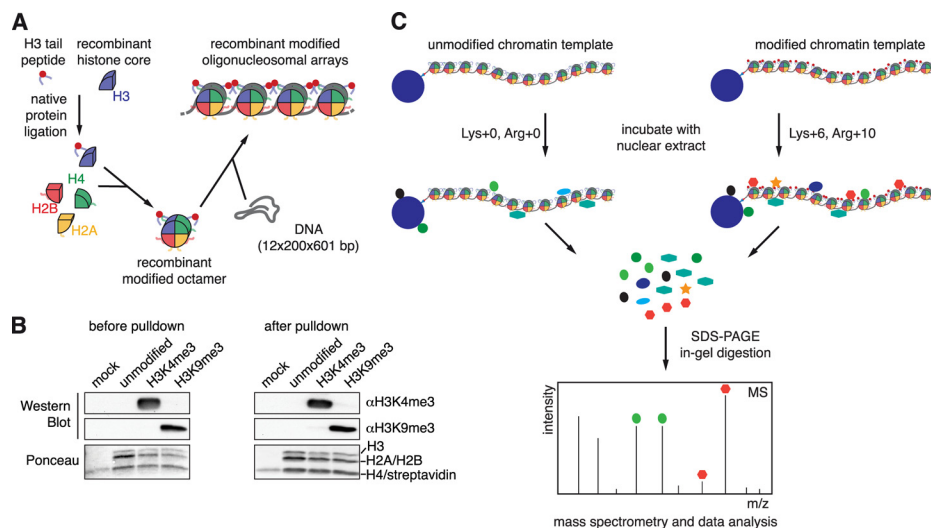
and deposited onto 5′ biotinylated 12 × 200 × 601 DNA template, which contains strong nucleosome positioning potential, using the salt dialysis method (23, 24). Material assembled with unmodified H3, H3K4me3, and H3K9me3 was analyzed by SDS-PAGE and via MNase digest confirming similar histone content and nucleosome density (supplemental Fig. S2). Additional biophysical analysis using analytical ultracentrifugation and atomic force microscopy verified identical hydrodynamic and structural behavior of the different chromatin templates (data not shown).

Biotinylated, reconstituted oligonuclesomes or synthetic peptides unmodified or containing the H3K4me3 or H3K9me3 modifications were immobilized on magnetic streptavidin beads and incubated with nuclear extract prepared from HeLa S3 cells grown under SILAC conditions. We used normal isotope containing L-lysine and L-arginine for preparing "light" extracts and heavy isotope labeled $^{13}C_6$-lysine (Lys+6) and $^{13}C_6{}^{15}N_4$-arginine (Arg+10) for generating "heavy" extracts. Extracts were analyzed in trial experiments to verify high synchronicity of "light" and "heavy" material (*i.e.* both extracts contain the same proteins and in the same amounts but only differ in the labeling of the proteins, supplemental Fig. S3). In forward experiments unmodified chromatin or peptide templates were incubated with "light" extracts, whereas corresponding H3K4me3 or H3K9me3 matrices were incubated with "heavy" extracts. In reverse experiments this order was swapped (label swap experiment).

Western blot analysis of the chromatin templates before and after incubation with extract verified the identity of the modifications (Fig. 1B). Importantly, no loss of H3K4me3 or H3K9me3 after exposure to nuclear extracts was observed. Similarly, mass spectrometric analysis verified identity of the histone H3 N-terminal peptides (data not shown).

Proteins specifically retained on the different matrices were recovered from the beads. Eluates were mixed in 1:1 ratio, run on SDS-PAGE gels and the separated proteins were trypsinized. The tryptic peptides were then analyzed by mass spectrometry and quantitative ratios for heavy and light SILAC pairs were determined (Fig. 1C). To minimize random variation, experiments were repeated twice (biological replicates) for each set-up, *i.e.* each combination of unmodified *versus* H3K4me3 or H3K9me3 was run twice in the forward and twice in the reverse direction. Each reaction was analyzed three times (technical replicates) on the mass spectrometer to maximize the probability of faithful identification of all factors in the samples.

H3K4me3 and H3K9me3 Interactomes—We analyzed a total of ca. 2000 factors in each of the affinity purification experiments out of approximately 5000 proteins present in the Hela S3 nuclear extract (data not shown). These include proteins specifically and unspecifically enriched on the streptavidin beads as well as the chromatin or peptide containing matrices (Fig. 2). By comparing unmodified and modified templates we detected factors enriched (*i.e.* preferentially binding modified *versus* unmodified) or excluded (*i.e.* preferentially binding unmodified *versus* modified) by the H3K4me3 and H3K9me3 modifications for chromatin as well as peptide-containing matrices to different degrees beyond this background. Applying a relatively stringent threshold of fourfold change, 59 of these were found enriched on H3K4me3 chromatin of which 32 were represented in forward and reverse experimental set-up. Conversely, 18 factors were found excluded from this matrix of which seven were found in both forward and reverse experiments (Table I, Fig. 2A). For the H3K4me3 peptide we found 71 factors enriched with 60 of these represented in forward and reverse experiments; 22 factors were excluded from this matrix with eleven found in forward and reverse experiments (Fig. 2B). For the H3K9me3 chromatin affinity purification we found 39 factors enriched by this modification of which 21 were represented in forward and reverse experiments; nine factors were found excluded from this matrix with two represented in forward and
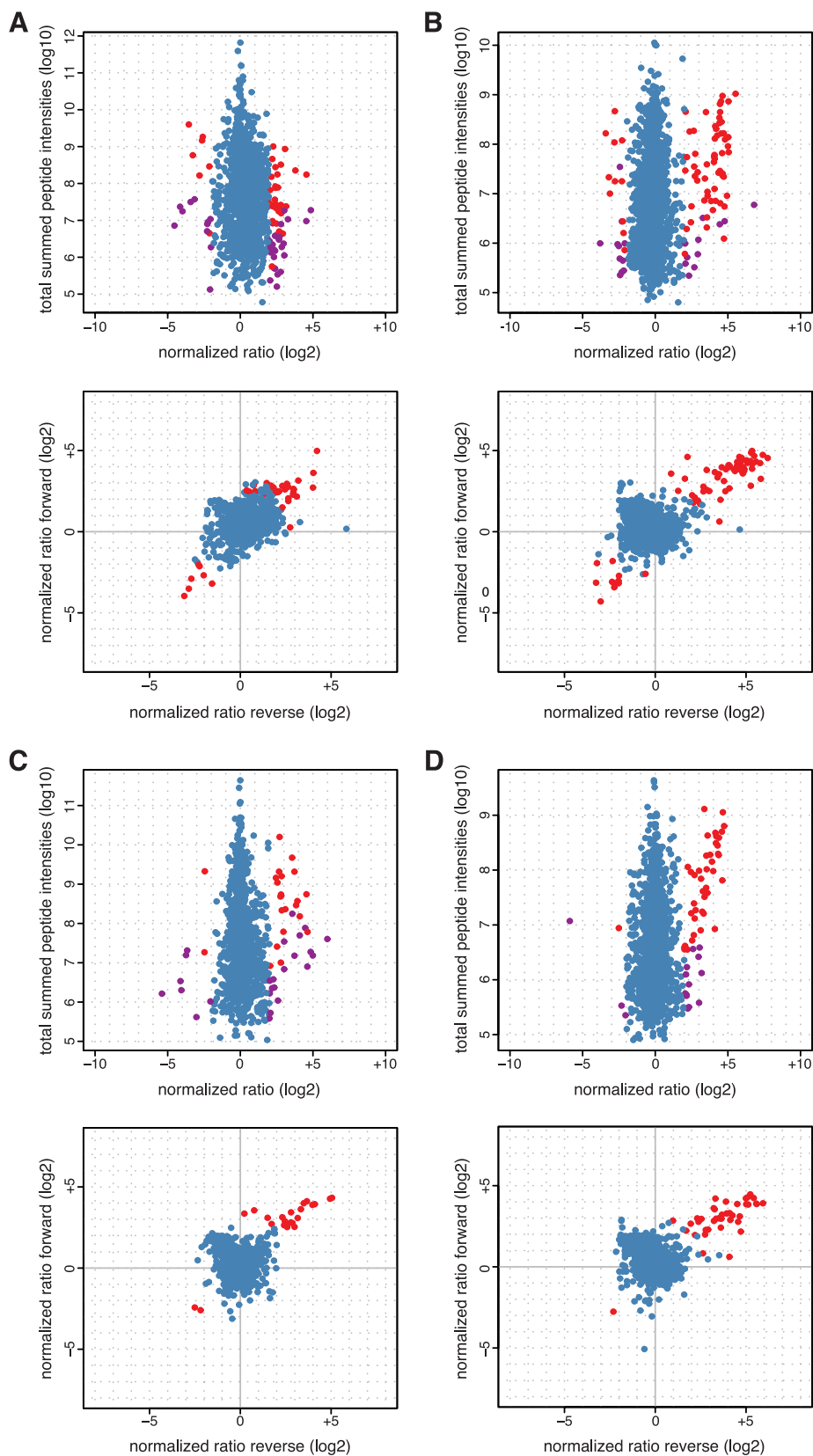
FIG. 2. **Identification of factors recruited by H3K4me3 or H3K9me3 using recombinant, uniformly modified chromatin or histone tail peptide affinity purification and SILAC-MS.** *A,* H3K4me3 chromatin. *B,* H3K4me3 histone tail peptide. *C,* H3K9me3 chromatin. *D,* H3K9me3 histone tail peptide. *Upper* panels: Scatter plots representing normalized ratios of identified and quantified proteins and total summed peptide intensities. Proteins identified in forward and reverse set-up of the experiment with ratio change above four are colored in *red*; those only identified in forward or reverse set-up of the experiment but with a ratio change above four are colored in *purple*. Factors with enrichment or exclusion ratios below four are colored in *blue*. Lower panels: Scatter plots representing normalized ratios of identified and quantified proteins in both, forward and reverse experiments. Proteins with ratio change above four are shown in *red*; those with enrichment or exclusion ratios below four are colored in *blue*. For details on the identified proteins see Tables I and II. In all plots proteins showing opposite ratios between forward and reverse experimental set-up (and therefore potential false positives) are omitted.

IPI number, gene name	Domains, motifs and regions of similarity[c]	Functional relevance[d]
H3K4me3		
Enriched with chromatin and peptide		
IPI00944951: TAF6	DUF1546, TAF	Transcription factor TFIID subunit
IPI00413755: TAF4	TAFH, TAF4	Transcription factor TFIID subunit
IPI00550655: SPIN1	Spin-Ssty	Cell cycle regulation
IPI00063434: PHF23*	PHD	
IPI00018108: TAF13*	TFIID-18kDa	Transcription factor TFIID subunit
IPI00018111: TAF7	TAFII55_N	Transcription factor TFIID subunit
IPI00004350: GTF2A1*	TFIIA	Transcriptional activation
IPI00853240: TAF3§ (29)	Bromo TP	Transcription factor TFIID subunit
IPI00480187: PHF8 (30)	JmjC, PHD	
IPI00872314: EMSY	ENT	Transcriptional repression
IPI00292750: PHF12	PHD	Transcriptional repression
IPI00298925: TAF5	TFIID_90kDa, WD40	Transcription factor TFIID subunit
IPI00645793: TAF1	Bromodomain, TBP-binding	Transcription factor TFIID subunit
IPI00607589: SIN3B	HDAC interact, PAH	Transcriptional repression, HDAC
IPI00018110: TAF11	TAFII28	Transcription factor TFIID subunit
IPI00018041: MAGEA3*	MAGE	
Enriched with chromatin		
IPI00297851: CHD1 (57)	Chromo, Helicase C, SNF2 N	ATP-dependand helicase
IPI00006651: SUPT7L	Bromo TP	STAGA complex subunit
IPI00010365: USP22	UCH, UBP zink finger	Ubiquitin carboxyl-terminal hydrolase
IPI00550119: SEPT6	Septin	Involved in cytokinesis
IPI00946738: FAM48A		Gastrulation regulation
IPI00005769: FANCG		DNA repair
IPI00009355: PARP12	PARP, CCCH zink finger	Poly [ADP-ribose] polymerase
IPI00009290: FANCF		DNA repair
IPI00444945: BAX	Bcl-2	Apoptosis regulation
IPI00014843: LRRC16A		Actin filament elongation
IPI00550523: ATL3	GBP	
IPI00016342: RAB7A	Ras	Endocytic transport
IPI00025202: FMNL1	Drf_FH3, Drf_GBD, FH2	Cell mobility and survival of macrophages
IPI00004859: BLM	BDHCT, DEAD, Helicase_C, HRDC, RQC	DNA replication and repair helicase
IPI00419575: C7orf20	DUF410	
IPI00022462: TFRC	PA, TFR dimer	Iron uptake
IPI00008986: SLC7A5	AA permease	Amino acid transport
IPI00300096: RAB35	Ras	Ras-related GTPase
IPI00175193: KIF4B	Kinesin	Cytokinesis
IPI00291510: IMPDH2	CBS, IMPDH	Regulation of nucleotide biosynthesis
IPI00031960: POLR1A	RNA_pol_Rpb1	rRNA synthesis
IPI00023608: FANCC	Fanconi C	DNA repair
IPI00152503: DTX3L	C3HC4 zink finger	Ubiquitin ligase
IPI00014977: MCM9	MCM	
IPI00004350: GTF2A1	TFIIA	Transcriptional activation
IPI00478737: RFWD3	WD40, C3HC4 zink finger	
IPI00008137: ZNF295	BTB, C2H2 zink finger	Transcriptional regulation
IPI00032496: MCM8	MCM	Cell proliferation control
IPI00022055: PCAF	Acetyltransf 1, Bromo, PCAF_N	Transcriptiopnal activating HAT
IPI00915456: DAXX	Daxx	Apoptosis regulation
IPI00885015: FANCL	WD-3	DNA repair ubiquitin ligase

T~ABLE~ I—*continued*

IPI00329737: FAAP24		DNA repair
IPI00386891: C17orf53	C2H2 zink finger	
IPI00171725: ZNF367	C2H2 zink finger	Transcriptional activation
IPI00176581: FANCM	DEAD, ERCC4, Helicase_C, ResIII	DNA repair ATPase
IPI00065356: CCDC111	DNA_primase_S, Herpes_UL52	
IPI00024236: GATA6	GATA, GATA N	Transcriptional regulation
IPI00060141: ZBTB9	BTB, C2H2 zink finger	Synaptic sygnaling
IPI00783133: METTL14	MT-A70	
IPI00296069: ARID4A	ARID, RBB1NT	
IPI00141118: EPC2	E Pc C, EPL1	Transcriprional regulation and DNA repair
IPI00178386: TTC21B	TPR 1	SHH signal transduction regulation
IPI00953051: KAT5	MOZ SAS (KAT5 = TIP60)	Transcriptional activating HAT
Enriched with peptide		
IPI00013885: CASP14	Peptidase C14	Epidermal differentiation
IPI00022831: TBP	TBP	Transcriptional activation
IPI00016930: ING2[#,§] (32)	PHD	HAT and HDAC regulation
IPI00166009: KDM2A	F-box, JmjC, CXXC zink finger	Histone lysine demethylase
IPI00171123: GATAD1	GATA	
IPI00373869: C17orf49		
IPI00607645: SUDS3	Sds3	Transcriptional repression
IPI00099385: ING1	PHD	Transcriptional regulation
IPI00031653: BRMS1L	Sds3	Transcriptional repression
IPI00170596: SIN3A	HDAC interact, PAH	Transcriptional repression
IPI00018510: SPIN2A	Spin-Ssty	Cell cycle regulation
IPI00785110: BPTF	Bromodomain, PHD	Transcriptional activation
IPI00002806: TAF12	TFIID-20kDa	Transcriptional activation
IPI00872208: TNRC18	BAH	
IPI00002993: TAF9	TFIID-31kDa	Transcriptional regulation
IPI00941164: TAF4B	TAF4, TAFH	Transcriptional regulation
IPI00021363: KDM5A	ARID, JmjN, PHD, PLU-1, C5HC2 zink finger	Histone lysine demethylase
IPI00002220: SAP130		Transcriptional repression
IPI00022019: SAP30		Transcriptional repression
IPI00065313: TAF8	Bromo TP, TAF8 C	Transcriptional activation
IPI00030364: TAF10	TFIID-30kDa	Transcriptional regulation
IPI00642105: TAF9B	TFIID-31kDa	Transcriptional regulation
IPI00328828: ARID4B	ARID, RBB1NT	Transcriptional repression
IPI00607848: BRMS1	Sds3	
IPI00002831: SAP30L		Transcriptional regulation
IPI00455982: HMGXB4	HMG box	
IPI00171309: PHF13	PHD	
IPI00061680: CCDC10	DUF1325	
IPI00008054: BRPF3	Bromodomain, PHD, EPL1, PWWP	
IPI00328144: TAF2	Peptidase M1	Transcriptional regulation
IPI00641026: CXXC1	PHD, CXXC zink finger	Transcriptional activation
IPI00639887: FAM60A		
IPI00398103:		Transcriptional regulation
IPI00847793: DCD		Pathogen defence
IPI00654744: SYNGR2	MARVEL	
IPI00028109: DPY30	Dpy-30	
IPI00914930: ANKRD11	Ank	Transcriptional regulation
IPI00867617: PHF2	JmjC, PHD	
IPI00550968: MORF4L1	MRG	Transcriptional activation
IPI00782935: ING5	PHD	Transcriptional regulation
IPI00922181: MCM2	MCM	Cell cycle regulation
IPI00743143: ING4	PHD	Transcriptional regulation
IPI00005492: WDR5 (33)	WD40	
IPI00006029: FOXK2	FHA, Fox head	Transcriptional regulation
IPI00180764: MYST2	MOZ SAS, C2HC zink finger	Transcriptional repression
IPI00292376: GMIP	C1 1, RhoGAP	

TABLE I—*continued*

IPI00412787: ARL5A	Arf	
IPI00004344: AFF4	AF-4	Transcriptional regulation
IPI00847436: KDM5B	ARID, JmjN, PHD, PLU-1, C5HC2 zink finger	Histone lysine demethylase
IPI00006077: PHF16	EPL1, PHD	
IPI00396967: FHL2	LIM	Transcriptional regulation
IPI00009373: EAF6	NuA4	
IPI00306794: CARD6	CARD	Apoptosis regulation
IPI00658062: ZNF131	BTB, C2H2 zink finger	Transcriptional regulation
Excluded from chromatin and peptide		
IPI00472782: PHF14 *	PHD	
IPI00604590: NME1-NME2 *	NDK	Nucleoside biosynthesis
Excluded from chromatin		
IPI00797279: UHRF1	PHD, ubiquitin, YDG SRA	Transcriptional regulation, ubiquitin ligase
IPI00296772: GGA2	Alpha adaptin C2, GAT, VHS	Protein sorting
IPI00003965: USP7	MATH, UCH	Ubiquitin carboxyl-terminal hydrolase
IPI00908444: CAMK2G	CaMKIID, Protein kinase	Potentiation and neurotransmitter release
IPI00031519: DNMT1	BAH, DMAP binding, DNA methylase, CXXC zink finger	CpG methylation, transcriptional repression
IPI00167031: IL34		Immune responce
IPI00748954:		
IPI00032313: S100A4	S100	Calcium binding
IPI00028618: MGMT	DNA binding 1, Methyltransferase 1N	DNA repair methyl transferase
IPI00294486: DUSP9	DSPc	MAP kinase phosphatase
IPI00216614: BCL2L10	Bcl-2	Apoptosis suppresion
IPI00328688: SCML2	MBT, SAM1	Transcriptional repression
IPI00329820: ACTL8	Actin	
IPI00291215: PARP14	Macro, PARP	Transcriptional regulation, ADP-ribosyltransferase
IPI00549725: PGAM1	PGAM	Core metabolism
IPI00157837: PHF19	PHD	Transcriptional repression
Excluded from peptide		
IPI00024719: HAT1	Hat1 N	Non-nucleosomal HAT
IPI00879166: MTA1	BAH, ELM2, GATA, Myb DNA binding	Transcriptional regulation
IPI00439194: MBD3	MBD	Transcriptional repression, meCpG binding
IPI00434623: MBD2	MBD	Transcriptional repression, meCpG binding
IPI00103554: GATAD2B	GATA	Transcriptional repression
IPI00171798: MTA2	BAH, ELM2, GATA, Myb DNA binding	Transcriptional regulation
IPI00018198: HAUS2		
IPI00744834: STX5	SNARE, Syntaxin	Vesicular transport
IPI00062037: DYNLL2	Dynein light	Intracelular transport and motility
IPI00020557: LRP1	EGF, EGF CA, Ldl recept A/B	Lipid metabolism
IPI00844507: C1orf174		
IPI00014376: RAB31	Ras	
IPI00026520: TM4SF1	L6 membrane	
IPI00465222: CHD3	Chromo, PHD, SNF2 N, Helicase C, CHDCT2, CHDNT, DUF1086/1087	Transcriptional regulation, helicase
IPI00478128: GATAD2A	GATA	Transcriptional repression
IPI00828172: FAM114A2	DUF719	
IPI00465028 TPI1	TIM	Core metabolism
IPI00852806:	Sec15	Vesicular transport
IPI00414985: C13orf27		
IPI00008986: SLC7A5	AA permease	Amino acid transport

[a] Only factors with a four-fold enrichment over the corresponding unmodified templates are given. Table entries are ranked according to the fold enrichment.

[b] Proteins are identified via the International Protein Index (IPI) number. Only one of in may cases several protein names are listed.

[c] Protein domains and motifs were derived from Pfam (56).

[d] Functional relevance according to STRING (54).

reverse experiments (Table II, Fig. 2*C*). With the H3K9me3 histone N-terminal tail peptide we found 53 factors enriched with 40 of these found in forward and reverse experiments; four factors were excluded by this modification on the peptide of which one was represented in forward and reverse experiments (Fig. 2*D*).

Factors found enriched or excluded on H3K9me3 chromatin and/or peptide templates from HeLa S3 nuclear extracts. [a, b, c, d] Factors in italics were identified only in forward or reverse set-up of the experiments. Asterisks mark factors that were identified in forward and reverse set-up of the experiment with either peptide or chromatin templates, but were only found in forward or reverse set-up of the experiment using the other matrix. Factors highlighted in red were verified as direct H3K9me3 binding proteins in independent biochemical experiments using recombinant proteins (please refer to the indicated references for study details). Factors highlighted in blue were also found in a recent SILAC MS study using modified mononucleosomes for affinity purification (46). Factors highlighted in green were also found in a recent SILAC MS study using histone tail peptides for affinity purification (6). Factors highlighted in brown were found overlapping in two recent SILAC MS studies, in histone tail peptide and mononucleosome based experiments (6, 46). Verified interaction factors that were not identified in a recent study using modified mononucleosomes for affinity purification are marked with § (46). Verified interaction factors that were not identified in a recent study using histone tail peptides for affinity purification are marked with # (6)

IPI number, gene name	Domains, motifs and regions of similarity[c]	Functional relevance[d]
H3K9me3		
Enriched with chromatin and peptide		
IPI00890837: SMCHD1	HATPase, SMC hinge	
IPI00022215: ADNP	Homeobox, C2H2 zink finger	Transcriptional regulation
IPI00878669: CBX1§ (34, 58)	Chromo, Chromo shadow	Epigenetic repression
IPI00297579: CBX3 (34, 58)	Chromo, Chromo shadow	Epigenetic repression
IPI00024662: CBX5 (34, 58)	Chromo, Chromo shadow	Epigenetic repression
IPI00845355: ATRX	Helicase C, SNF2 N	Transcriptional regulation
IPI00410720: POGZ	CenpB DNA binding, DDE, C2H2 zink finger	
IPI00011857: CHAF1B	WD40	Chromatin assembly
IPI00023177: CHAF1A		Chromatin assembly
IPI00797279: UHRF1# (35)	PHD, ubiquitin, YDG SRA	Transcriptional regulation, ubiquitin ligase
IPI00641109: ZMYM3	FCS zink figer	
IPI00477949: ZMYM4	FCS zink figer	
IPI00044681: UHRF2	PHD, ubiquitin, YDG SRA, C3HC4 zink finger	Transcriptional regulation, ubiquitin ligase
IPI00436632: NIPBL		Chromatid cohesion
IPI00064212: ZNF828	C2H2 zink finger	
IPI00915456: DAXX	Daxx	Apoptosis regulation
IPI00479789: C1orf103		
IPI00294603: ZMYM2*	FCS zink figer	Transcriptional regulation
IPI00000656: KIAA0892	Cohesin load	
IPI00329820: ACTL8	Actin	
Enriched with chromatin		
IPI00025753: DSG1	Cadherin, Cadherin C	Cell-cell contacts
IPI00010948: TRIM26	SPRY, B-box zink finger, C3HC4 zink finger	
IPI00410287: PRKAA1	Protein kinase	Lipid metabolism
IPI00913848: FERMT2	Ferm M, PH	Cytoskeleton dynamics
IPI00852685: DIAPH1	Drf DAD/FH1/FH3/GBD, FH2	Actin filament regulation
IPI00397904: NUP93	Nic96	Nuclear pore assembly
IPI00402657: RPAP1	RPAP1 C/N	Transcriptional regulation
IPI00219518: ARL1	Arf	Phospholipase D activation
IPI00397801: FLG2	Efhand, Flaggirin, S100, SVS QK	
IPI00947285:		
IPI00004317: POLG	DNA Pol A	Mitochondrial DNA replication
IPI00216099: DSC1	Cadherin, Cadherin Pro	Cell-cell contacts
IPI00026256: FLG	Flaggirin, S100	Epidermal differentiation
IPI00103242: POF1B		Ovary development
IPI00878849: P2RX5	P2X receptor	Rho/Wnt signaling regulation
IPI00021536: CALML5	Efhand	Calcium binding
IPI00071509: PKP1	Arm	Cell-cell contacts
IPI00009949: PSMF1	PI31 Prot reg	Proteasome inhibition
IPI00009777: ZNF581	C2H2 zink finger	Transcriptional regulation
Enriched with peptide		
IPI00438229: TRIM28	PHD, B-box zink finger, C3HC4 zink finger	Transcriptional repression
IPI00402209: ADNP2		Transcriptional regulation
IPI00855833: PRR12		
IPI00396015: ACACA	ACC central, Biotin carb C, Biotin lipoyl, Carboxyl trans, CPSase L chain, CPSase L D2	Core metabolism
IPI00010252: TRIM33	Bromodomain, PHD, B-box zink finger	Transcriptional repression

TABLE II—*continued*

IPI00293963: CDYL (22)	Chromo, ECH	Transcriptional repression
IPI00455210: CHD4	PHD, Chromo, CHDCT2, CHDNT, \DUF1086/1087, Helicase C, SNF2 N	Transcriptional regulation
IPI00021700: PCNA	PCNA C/N	DNA replication
IPI00843937: KIAA0892)	Cohesin load	
IPI00149044: ZNF280D	C2H2 zink finger	Transcriptional regulation
IPI00024502: UBQLN4	UBA, ubiquitin	
IPI00400826: CLU	Clusterin	Apoptosis
IPI00031519: DNMT1	BAH, DMAP binding, DNA methylase, CXXC zink finger	CpG methylation, transcriptional repression
IPI00924574: APOD	Lipocalin	Lipid transport
IPI00217540: KDM1	Amino oxidase, SWIRM	
IPI00743157: WHSC1L1	PHD, PWWP, SET	Transcriptional regulation
IPI00477303: HOMEZ	Homeobox	Transcriptional regulation
IPI00888042: ZNF316	KRAB, C2H2 zink finger	Transcriptional regulation
IPI00885104: MPHOSPH8[§] (37)	Ank, Chromo	
IPI00008531: RCOR1	ELM2, Myb DNA binding	Transcriptional repression
IPI00019329: DYNLL1	Dynein light	Intracellular transport and motility
IPI00514648: SMARCA2	BRK, Bromodomain, Helicase C, HAS, QLQ, SNF2 N	Transcriptional activation
IPI00642271: SLC35B2	UAA	PAPS transport, MAPK and NFkB activation
IPI00639924: C19orf68	FAR1	
IPI00003965: USP7	MATH, UCH	Ubiquitin carboxyl-terminal hydrolase
IPI00019520: ZNF192	KRAB, SCAN, C2H2 zink finger	Transcriptional regulation
IPI00002549: ANAPC2	APC2, Cullin	Cell cycle regulation
IPI00002441: SDC1	Syndecan	Cell contact
IPI00419402: ZNF8	KRAB, C2H2 zink finger	Transcriptional regulation
IPI00302755: RBAK	KRAB, C2H2 zink finger	Transcriptional regulation
IPI00306446: ZNF24	SCAN, C2H2 zink finger	Transcriptional regulation
IPI00410039: PPHLN1		Epidermal differentiation
Excluded from chromatin		
IPI00396015: ACACA	ACC central, Biotin carb C, Biotin lipoyl, Carboxyl trans, CPSase L chain, CPSase L D2	Core metabolism
IPI00219806: S100A7	S100	Calcium binding
IPI00022204: SERPINB3	Serpin	Immune response
IPI00909649: IGKC	C1-set, V-set	Immune response
IPI00219757: GSTP1	GST C/N	Glutathione conjugation
IPI00010303: SERPINB4	Serpin	Immune response
IPI00028004: PSMB3	Proteasome	Proteasome regulation
IPI00291215: PARP14	Macro, PARP	Transcriptional regulation, ADP-ribosyltransferase
IPI00852669: ZNF516	C2H2 zink finger	Transcriptional regulation
Excluded from peptide		
IPI00183606: CYP2W1	p450	
IPI00154283: KIAA1524		Myc stabilizing oncoprotein
IPI00016339: RAB5C	Ras	Vesicular traffic
IPI00639982: DYNLT3	Tctex 1	

[a] Only factors with a four-fold enrichment over the corresponding unmodified templates are given. Table entries are ranked according to the fold enrichment.

[b] Proteins are identified via the International Protein Index (IPI) number. Only one of in may cases several protein names are listed.

[c] Protein domains and motifs were derived from Pfam (56).

[d] Functional relevance according to STRING (54).

The different data sets contain factors that have been shown to directly interact with H3K4me3 or H3K9me3 in independent biochemical experiments, thereby validating our approach. TAF3 (29), PHF8 (30), CHD1 (31), ING2 (32), and WDR5 (33) are known H3K4me3 interacting proteins. The HP1 isoform proteins CBX1, CBX3, CBX5 (34), as well as UHRF1 (35), CDYL1 (36), and MPHOSP8 (37) have been shown to bind H3K9me3. Besides direct interaction partners, the data sets also include proteins that are known to be indirectly re-cruited to the chromatin marks. For example, TFIID components (*e.g.* TAF1–2, 4–13) are recruited to H3K4me3 via TAF3 (29). POGZ is bound to H3K9me3 via CBX5 (38). Known or predicted functional interactions between the identified enriched proteins are shown in supplemental Fig. S4. Additional work will be necessary to investigate which of the newly identified components interact directly or indirectly with the chromatin marks.

Overall, the data present a significant expansion of the repertoire of factors that are recruited to H3K4me3 or

H3K9me3 chromatin marks. Nevertheless, it is clear that use of other procedures for preparing extracts as well as different cellular sources (cell type, stage of differentiation) will produce distinct data sets. Applying a lower threshold, the overall number of factors identified using standard Hela S3 nuclear extract is much larger (see supplemental Tables S1–S4 for raw data). However, we feel that a fourfold change presents a robust signal and therefore focused for further analysis on this data set. Analysis of the data using values of significance ("B") as calculated by the MaxQuant software with a cutoff of 0.05 is shown in supplemental Fig. S5 (39).

We ascribe the fact that around 36% of all factors specifically identified in this study reveal high enrichment or exclusion ratios only in forward or reverse experiments but not in both to the high threshold level of fourfold that we set for the analysis. In fact, detailed examination of the proteins only enriched or excluded in the forward or reverse set-up of the experiment showed that these are largely factors that are more difficult to identify (*i.e.* these have a lower summed peptide total intensity; see purple colored hits in Fig. 2). Low abundance in the extract, small protein size yielding few peptides, and peptide hydrophobicity might contribute to this phenomenon. Also, batch to batch variability of extracts might play a role in factors only identified in forward or reverse experiments. We tried to minimize this possibility by carefully matching the different extracts used (supplemental Fig. S3). Last, false negative identification (*i.e.* a factor was by chance not detected in forward or reverse experiment) might be a relevant factor in the analysis. Although proteins identified by both forward and reverse experimental set-up present the most stringent hits, proteins that are found in forward or reverse experiments nevertheless result from averages of four independent experiments (two times forward and two times reverse, see above). A number of factors were also represented only in forward or only in reverse set-up of the experiment using either chromatin or peptide templates, but were identified in both directions of the experiment using the other matrix (annotated with asterisk in Tables I and II). We think that these are therefore meaningful candidates and included them in our further analysis.

Fig. 2 also shows that there is general good agreement between proteins identified in forward and reverse experiments. Interestingly, more factors are enriched than excluded by the H3K4me3 and H3K9me3 histone modifications both, in the context of chromatin as well as peptides. While our type of analysis excludes factors that bind histone H3 irrespective of H3K4me3 or H3K9me3 modifications, we do not think that this observation is caused by a technical problem of the method, but rather presents a "true" finding. The available structural data on different histone modification binding proteins identify highly specialized and in many cases narrow binding pockets where multiple interactions mediate recognition and binding of the PTMs (7). This binding mode likely generates a bigger change in free energy than is achieved by a PTM that is added to a stretch of amino acids recognized by a larger protein surface in the unmodified state. Therefore, the attractive mode might generate more discrimination than the repelling mode. Although additional experiments are necessary to test this hypothesis, we nevertheless note that when going from lower to higher eukaryotes the number and type of histone modifications significantly increases. This phenomenon might reflect the fact that the attractive mode indeed generates more robust signal transduction.

Validation of the Approach—To assess the quality of the new data sets of H3K4me3 and H3K9me3 interacting factors, we choose to independently analyze a set of proteins from each category that had not been analyzed in this context before. We transiently expressed candidate factors in 293 HEK cells and performed peptide or chromatin affinity purification experiments that were analyzed by Western blotting against an engineered FLAG-tag on all factors. As Fig. 3*A* shows, SPIN1 a factor that is implicated in cell cycle regulation (40) was recovered on the peptide and chromatin H3K4me3 templates, but not on the corresponding unmodified matrices, thereby essentially verifying the results from the SILAC MS analysis. Similarly, we found FANCF, a factor of the Fanconi anemia group (41) specifically enriched on the H3K4me3 chromatin template, but not the corresponding peptide matrix as we had seen in the SILAC MS. Of the H3K9me3 binding factors ADNP, which is a protein containing a neuroactive peptide but that has also nuclear functions (42), and ZMYM3, a Zn-finger protein of unknown function (43) bound specifically to the H3K9me3 peptide and chromatin templates as we had detected in the SILAC MS analysis (Fig. 3*B*). In contrast, ACTL8, an actin-like protein of unknown function, did not reproduce the findings from the SILAC-MS. We detected the overexpressed protein in comparable amounts bound to the unmodified and H3K9me3 templates. Although this finding might identify a false positive of our screening procedure, we nevertheless point out that ACTL8 contains a PSVLL motif. PxVxL motifs in other proteins have been found to interact with factors of the HP1 type that directly bind H3K9me3 (44). Additional experiments need to find out whether ACTL8 indeed can interact with HP1 and whether overexpression and/or tagging of this factor interfere with its biology. Lastly, we used a specific antiserum against SMCHD1, a factor that might be implicated in the structural maintenance of chromosomes and that was recently found enriched at telomeres (45) to verify that the endogenous, cellular protein is recruited to H3K9me3 (Fig. 3*B*).

Because the nuclear distribution of H3K4me3 and H3K9me3 are very different, we also analyzed the localization of the new candidate histone methyl-lysine interacting factors in NIH3T3 cells. Here, we found transiently expressed SPIN1 and FANCF diffusely spread in the cell nucleus in a pattern that was reminiscent of H3K4me3 distribution (Fig. 3*C*). In contrast, transiently expressed ADNP
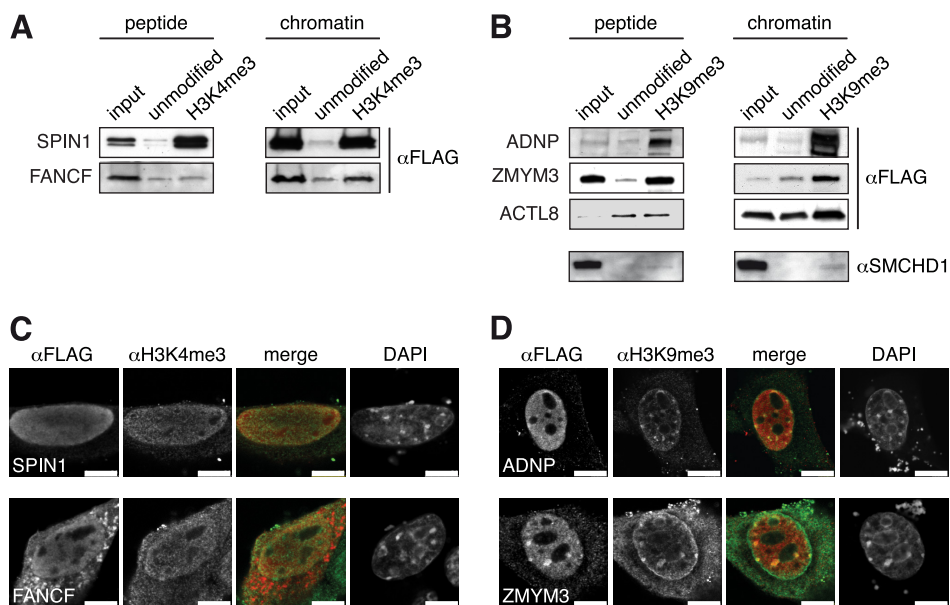
FIG. 3. **Verification of H3K4me3 and H3K9me3 interacting factors.** *A* and *B*, The indicated proteins containing C-terminal FLAG-tags were transiently expressed in 293T cells. Peptide or chromatin affinity purifications using H3K4me3 (*A*) or H3K9me3 (*B*) templates were performed from nuclear extracts and analyzed by Western blot using anti-FLAG antibodies. In case of SMCHD1 extract from untransfected cells was used and the respective affinity purifications were analyzed using anti-SMCHD1 antibodies. Input, 2%. *C* and *D*, The indicated proteins containing C-terminal FLAG-tags were transiently expressed in NIH3T3 cells. Immunofluorescence analysis was carried out using anti-FLAG and anti-H3K4me3 (*C*) or anti-H3K9me3 (*D*) antibodies. Merged images correspond to the overlay of the two different antibody stainings. DNA was stained with DAPI. Scale bar represents 7.5 μm.

and ZMYM 3 showed enrichment at discrete nuclear foci besides diffuse general localization. As these foci were marked by H3K9me3 and are DNA rich, these represent pericentric heterochromatin. Overall, the results verify five out of six candidates tested as novel interaction partners of H3K4me3 or H3K9me3.

Interestingly, only SPIN1 and ADNP, but neither FANCF, ZMYM3, nor SMCHD1 were found in recent histone tail peptide (6) or mononucleosome (46) H3K4me3 and H3K9me3 affinity purification experiments. Although there is clearly some overlap with the data sets of the peptide based studies (see Tables I and II) the differences of the mononucleosome- and our oligonucleosme-based studies are striking. As the mononucleosome-based data were already analyzed with a very low twofold cutoff of enrichment, these findings might indicate that multiple nucleosomes in the form of arrays provide different and potentially better landing platforms for factors binding to chromatin marks. Although we do not know the basis for the discrepancies in the separate studies, we note that both previously published experiments (6, 46) performed fewer biological replicates, analyzed the data with far lower enrichment cutoffs and did not provide data on the quality of the SILAC extracts used. Additional work is required to resolve potential technical differences in the different studies and to assess the overall quality of the data sets provided.

Comparison of H3K4me3 and H3K9me3 Interactomes— There is generally no correlation of the factors identified

with the H3K4me3 and the H3K9me3 histone PTMs, which reflects the different biological contexts that these modifications have been implicated in (Fig. 4*A*). Only a few proteins were identified in both, the H3K4me3 and H3K9me3 data sets (*e.g.* DAXX), but then only with chromatin or peptide templates (DAXX was identified only on chromatin with H3K4me3, but on chromatin and peptide templates with H3K9me3). These might represent factors that have a general affinity for tri-methylated lysine residues irrespective of sequence context. Promiscuous binding to (mono- and di-) methyl-lysine marks in different histone sequence environments has for example been observed for proteins containing malignant brain tumor domains (47).

Several proteins (*e.g.* DNMT1, UHRF1) show enrichment with one but exclusion with the other modification. Although these are only represented in either the peptide or chromatin data sets using the stringent fourfold cutoff (*e.g.* DNMT1 was found enriched not only on the H3K9me3 peptide, but also the H3K9me3 chromatin, but with a 3.7 ratio), such factors could be of high biological interest as they might reflect proteins that mediate binary switches between different totally exclusive chromatin states. On a global level, binary chromatin domains have been described for the activating H3K4me3 and repressing H3K27me3 histone PTMs, where regions that contain both chromatin marks in the pluripotent cell state resolve during differentiation into either of the two states (48).

Interestingly, we find far more factors excluded by H3K4me3 chromatin and peptide templates compared with the H3K9me3 PTM (see Fig. 2). This might indicate that gen-
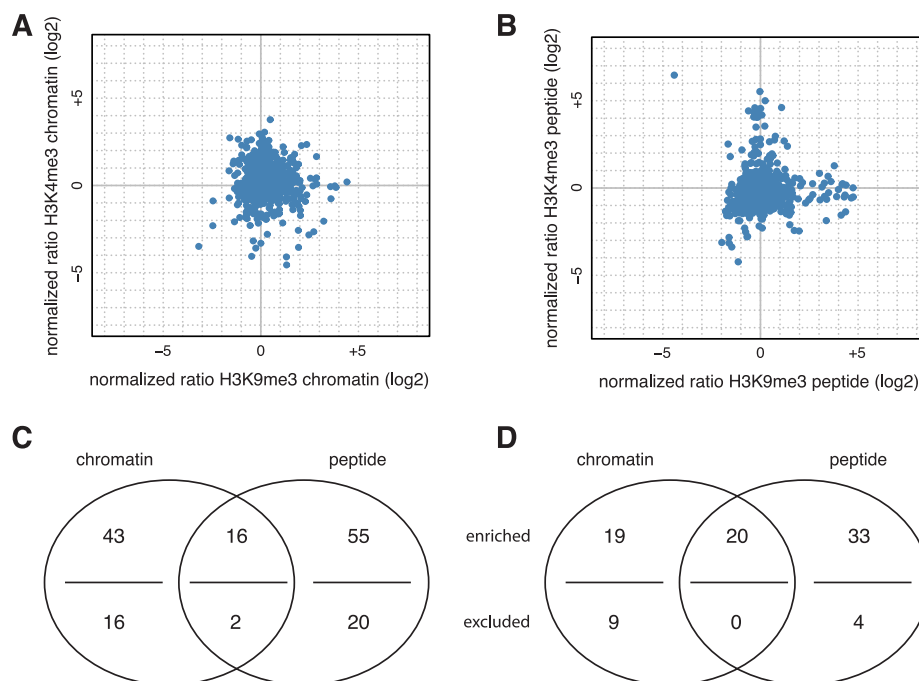
Fig. 4. **Overall evaluation of chromatin and histone tail peptide H3K4me3 and H3K9me3 affinity purifications.** Comparison between H3K4me3 and H3K9me3 interactomes in the context of chromatin (*A*) and peptide (*B*) affinity purification reactions. Only proteins identified with both modifications are plotted. Chromatin and peptide affinity purifications identify distinct as well as overlapping sets of proteins recruited to H3K4me3 (*C*) and H3K9me3 (*D*). Venn diagrams show the number of factors identified with each approach with a fourfold cutoff, both enriched with the specific modification (*above* line) and excluded by the modification thereby preferentially binding to the unmodified template (*below* line).

erally more factors can bind to the unmodified very N-terminal region of H3 compared with the H3K9 context. We wonder whether this phenomenon reflects the fact that in higher eukaryotes the default chromatin state is repressive (49). The list of factors excluded by H3K4me3 indeed contains some proteins, which according to gene ontology are implicated in transcriptional repression. Comparison of the interactomes of additional activating and repressive chromatin marks might provide further insights into this behavior.

Comparison of Chromatin and Peptide Affinity Purifications—The total numbers of factors identified by the chromatin or peptide affinity purifications for the H3K4me3 and the H3K9me3 PTMs are quite similar (Fig. 4*B*). However, the degree of overlap between the proteins recruited by the corresponding chromatin and peptide templates is rather limited. A far larger number of factors are identified only by the peptide-based approach or only by the chromatin-based approach. In light of the fact that both, H3K4me3 and H3K9me3 modifications are very distal from the H3 core domain (the H3 tail region encompasses the first 36 amino acids, ref. 50) and are thereby at the periphery of the nucleosome this finding is rather surprising. A priori one might expect to identify the same factors with both approaches and to potentially recruit and recover more proteins on the chromatin templates. After all, additional interaction surfaces (*e.g.* DNA, other histone tail and core regions) are available in this native setting. By and large, both approaches might be highly complementary. Future

studies will need to tell whether the candidates identified with either approach are more functionally relevant than the other. However, the context of patterns of chromatin modifications especially in the context of DNA methylation as well as in a trans-histone setting can certainly only be investigated by the chromatin-based approach.

For each histone PTM we identified slightly more factors with the peptide templates compared with the chromatin templates. We think this might be a reflection of the potentially higher substitution rate of the peptides on the magnetic streptavidin beads. For immobilization of chromatin representing the same amount of free H3 tails far more beads are needed. Likely, there is steric exclusion on the streptavidin tetramer as well as on the bead surface by the chromatin complex. Also, binding of factors to histone PTMs in the context of chromatin might be subject to repulsive forces by DNA as well as steric hindrance thereby fine-tuning the binding of proteins or multiprotein complexes. Last, we do not know whether the histone tails are fully available on the surface of the nucleosomes in general or under the experimental buffer conditions used (51).

In the case of peptide affinity purifications, a stronger tendency of detecting a protein with one modification as not enriched (1:1 ratio of unmodified to modified templates) and in the other modification as enriched can be seen compared with the chromatin affinity purifications (see Fig. 4*A*, clouds along the axes). Obviously, the chromatin environment presents the more stringent and more discriminating binding surface.

Although the data sets of the H3K9me3 peptide and chromatin affinity purifications as well as the H3K4me3 peptide affinity purifications show a similar overall distribution with relative narrow and focused clustering of the background (blue dots in Fig. 2) as well as distinct highly enriched or excluded factors (red dots in Fig. 2), the results of the H3K4me3 chromatin affinity purification appear different. Here, the background shows an overall wider distribution and only very few factors with high change ratios were identified. Because the results of the H3K4me3 peptide affinity purification are different, this distinction cannot be caused by the histone PTM itself, but must be a consequence of embedding this methyl-lysine mark in a chromatin context. Although we have so far not detected any difference in the biochemical and biophysical behavior of the unmodified, H3K4me3 or H3K9me3 recombinant chromatin preparations, the accessibility of the histone H3 tail might be limited by lysine 4 tri-methylation. This might be a nucleosome restricted effect or be caused by overall chromatin conformational properties (*i.e.* compaction status). Indeed, single histone modifications affecting the overall behavior of recombinant chromatin templates have been described (52).

Distinct Protein Domains Mediate Recruitment to H3K4me3 and/or H3K9me3—To gain further insight into the recruitment of factors to histone methyl-lysine marks we performed clustering analysis focusing on protein domains (Fig. 5). Prominent chromatin associated protein regions and motifs are highly enriched on the histone methyl-lysine marks. These include several domains directly implicated in methyl-lysine recognition: chromo, PHD, SRA. Also, domains that provide binding interfaces for recruitment of additional proteins are visible *e.g.* chromoshadow. Other motifs like PxVxL, which has been shown to bind to the chromoshadow domain of HP1 proteins (44, 53), are present in factors presumably indirectly recruited via binding to factors directly interacting with the histone methyl-lysine marks. Common background proteins (ribosomal proteins, tubulins) are present within the middle cutoff group, as are some domains specific for chromatin (helix-loop-helix), peptide (HAT) or both 14-3-3, regardless of the modification used.

Although we detect domains that have been implicated in the general context of chromatin (*e.g.* bromodomains interacting with histone acetylation marks, SNF2 present in nucleosome remodeling factors), DNA (*e.g.* Zn fingers of various type, PLU-1, ARID, Myb, SANT) or methylated DNA (*e.g.* methyl-CpG binding domain), these are novel in the context of histone methyl-lysine marks. It will have to be seen which of these domains are direct histone methyl-lysine mark binding regions and which mediate additional protein-protein interactions in an indirect mode of recruitment. Also, domains that make contact to DNA or other histone regions of the nucleosome might stabilize weaker interactions with sensitivity to and discrimination of the histone PTMs. Analysis for functional interactions using STRING indeed indicates connection groups between several of the identified factors (sup-
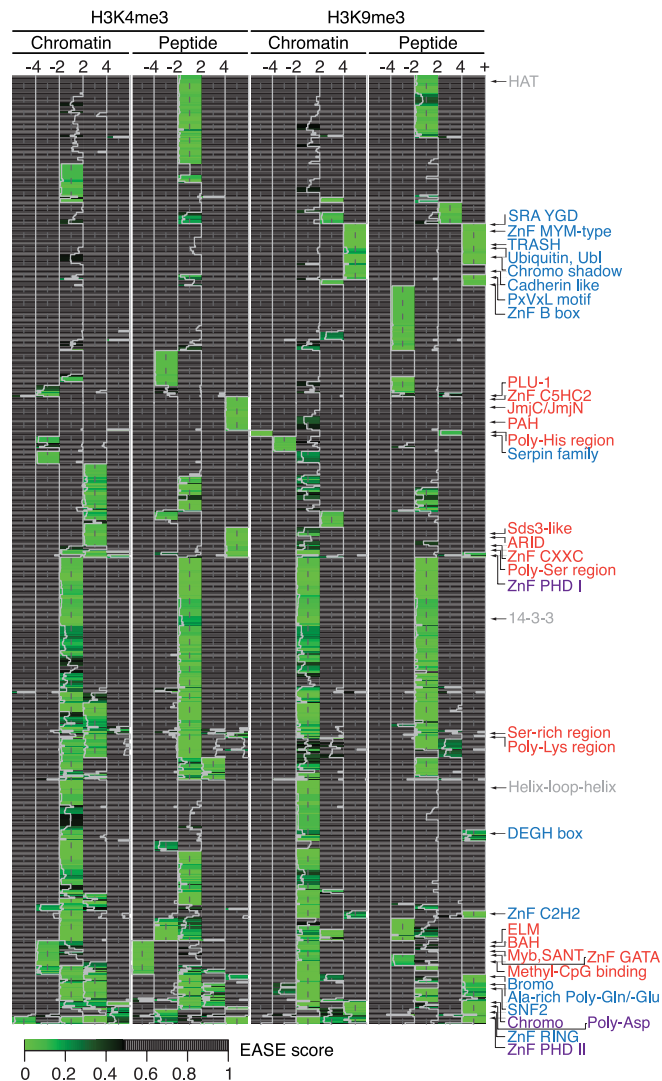
FIG. 5. **Domain enrichment in affinity purification reactions comparing H3K4me3 and H3K9me3 PTMs using chromatin and peptide templates.** Heatmap representing protein functional and structural domains and motifs enriched within each of the five indicated ratio cutoff groups (databases used: UniProt Sequence Feature, InterPro, PIR Superfamily, PFAM, SMART). Categories enriched or excluded (with a ratio of at least four) by H3K4me3 (*red*), H3K9me3 (*blue*) or both (*purple*) are annotated.

plemental Fig. S4) (54). For example, recruitment of the TFIID complex components has been described via TAF3 binding H3K4me3 (29). Another prominent interaction cluster here is between proteins from the Fanconi anemia group, implicated in the DNA damage response (41). Several of the enriched protein domains might function in the translation of the histone PTMs. This might involve enzymatic activities (*e.g.* JmjC/JmjN domains in histone demethylases) as well as regions directly impacting onto chromatin structure.

Interestingly, some protein regions are enriched on both, H3K4me3 and H3K9me3 PTMs (*e.g.* ZnF, PHD, chromo) while being structural and functional parts of different proteins.

Obviously, here the domains have evolved to recognize (tri-) methylated lysine residues in different sequence context, but with high discrimination against the unmodified state exemplifying the multiple use of successful and efficient protein folds and motifs.

CONCLUSIONS

Combination of affinity purification experiments of synthetic peptides representing different histone PTMs either in isolation or in the context of chromatin and quantitative mass spectrometric analysis using SILAC provides a comprehensive set of factors potentially mediating the readout and translation of these marks. Our results show that chromatin affinity purification largely defines a set of factors distinct from what can be found with modified histone tail peptides. We think this might be a general finding as comparison of similar analysis recently performed on histone tail peptides (6) or mononucleosomes (46) even show less overlap of factors recruited to different methyl-lysine marks (see also Tables I and II). The chromatin templates provide the advantage of offering additional binding interfaces such as DNA, histone core, other histones and/or other chromatin marks. Thereby, they potentially enable recruitment of multiprotein machineries making several independent contacts to chromatin. Future experiments have to show whether the chromatin data sets indeed contain functionally more relevant factors. In any case, our combined data sets of H3K4me3 and H3K9me3 chromatin and peptide affinity purifications paves the way for additional studies investigating the exact role of the identified proteins in recognition of these methyl-lysine marks as well as in directing chromatin structure and function. Here, combination with array-based technologies that allow screening of direct interactions provides an orthogonal technology (3, 5). Despite characterization of direct interactions with the chromatin marks, emphasis needs to be put onto multiprotein assemblies and interplay of factors that are recruited indirectly. Our global analysis of the protein domains enriched on the chromatin marks as well as the biological connection of factors based on STRING analysis provides a starting point.

Multiple factors might translate individual chromatin marks in different functional settings. In this context, interplay with other histone modifications as well as DNA methylation could manifest an important regulatory mechanism, which has been proposed in the histone code hypothesis (10). Indeed, it is emerging that combinations of chromatin marks mark different domains of chromatin. For example, pericentromeric heterochromatin in higher eukaryotes is enriched in H3 lysine 9 trimethylation (H3K9me3), H4 lysine 20 trimethylation (H4K20me3), H3 lysine 27 monomethylation (H3K27me1) as well as DNA methylation. Linkage to H3 arginine 2 dimethylation (H3R2me2) and H4 arginine 3 dimethylation (H4R3me2) has also been described (55). The use of uniformly modified, recombinant chromatin templates containing different combinations and patterns of chromatin marks for affinity purification experiments will provide an excellent starting point to define the complement of factors that mediate the functional status of such chromatin regions, whose biochemistry has been elusive for a long time.

REFERENCES

1. Fischle, W., Wang, Y., and Allis, C. D. (2003) Histone and chromatin cross-talk. *Curr. Opin. Cell Biol.* **15,** 172–183
2. Campos, E. I., and Reinberg, D. (2009) Histones: annotating chromatin. *Annu. Rev. Genet* **43,** 559–599
3. Bua, D. J., Kuo, A. J., Cheung, P., Liu, C. L., Migliori, V., Espejo, A., Casadio, F., Bassi, C., Amati, B., Bedford, M. T., Guccione, E., and Gozani, O. (2009) Epigenome microarray platform for proteome-wide dissection of chromatin-signaling networks. *PLoS One* **4,** e6789
4. Chan, D. W., Wang, Y., Wu, M., Wong, J., Qin, J., and Zhao, Y. (2009) Unbiased proteomic screen for binding proteins to modified lysines on histone H3. *Proteomics* **9,** 2343–2354
5. Liu, H., Galka, M., Iberg, A., Wang, Z., Li, L., Voss, C., Jiang, X., Lajoie, G., Huang, Z., Bedford, M. T., and Li, S. S. (2010) Systematic identification of methyllysine-driven interactions for histone and nonhistone targets. *J. Proteome Res.* **9,** 5827–5836
6. Vermeulen, M., Eberl, H. C., Matarese, F., Marks, H., Denissov, S., Butter, F., Lee, K. K., Olsen, J. V., Hyman, A. A., Stunnenberg, H. G., and Mann, M. (2010) Quantitative interaction proteomics and genome-wide profiling of epigenetic histone marks and their readers. *Cell* **142,** 967–980
7. Taverna, S. D., Li, H., Ruthenburg, A. J., Allis, C. D., and Patel, D. J. (2007) How chromatin-binding modules interpret histone modifications: lessons from professional pocket pickers. *Nat. Struct. Mol. Biol.* **14,** 1025–1040
8. Adams-Cioaba, M. A., and Min, J. (2009) Structure and function of histone methylation binding proteins. *Biochem. Cell Biol.* **87,** 93–105
9. Fischle, W., Wang, Y., and Allis, C. D. (2003) Binary switches and modification cassettes in histone biology and beyond. *Nature* **425,** 475–479
10. Jenuwein, T., and Allis, C. D. (2001) Translating the histone code. *Science* **293,** 1074–1080
11. Sims, R. J., 3rd, and Reinberg, D. (2008) Is there a code embedded in proteins that is based on post-translational modifications? *Nat. Rev. Mol. Cell Biol.* **9,** 815–820
12. Ruthenburg, A. J., Li, H., Patel, D. J., and Allis, C. D. (2007) Multivalent engagement of chromatin modifications by linked binding modules. *Nat. Rev. Mol. Cell Biol.* **8,** 983–994
13. Fischle, W., Tseng, B. S., Dormann, H. L., Ueberheide, B. M., Garcia, B. A., Shabanowitz, J., Hunt, D. F., Funabiki, H., and Allis, C. D. (2005) Regu-

lation of HP1-chromatin binding by histone H3 methylation and phosphorylation. *Nature* **438,** 1116–1122

14. Liu, H., Lin, D., and Yates, J. R., 3rd (2002) Multidimensional separations for protein/peptide analysis in the post-genomic era. *BioTechniques* 32, 898, 900, 902 passim

15. Wilm, M. (2009) Quantitative proteomics in biological research. *Proteomics* **9,** 4590–4605

16. Ong, S. E., and Mann, M. (2006) A practical recipe for stable isotope labeling by amino acids in cell culture (SILAC). *Nat. Protoc.* **1,** 2650–2660

17. Dignam, J. D., Martin, P. L., Shastry, B. S., and Roeder, R. G. (1983) Eukaryotic gene transcription with purified components. *Methods Enzymol.* **101,** 582–598

18. Biancalana, S., Hudson, D., Songster, M. F., and Thompson, S. A. (2001) Fmoc chemistry compatible thio-ligation assembly of proteins. *Lett. Peptide Sci.* **7,** 291–297

19. Futaki, S., Sogawa, K., Maruyama, J., Asahara, T., Niwa, M., and Hojo, H. (1997) Preparation of peptide thioesters using Fmoc-solid-phase peptide synthesis and its application to the construction of a template-assembled synthetic protein (TASP). *Tetrahedron Letters* **38,** 6237–6240

20. von Eggelkraut-Gottanka, R., Klose, A., Beck-Sickinger, A. G., and Beyermann, M. (2003) Peptide (alpha)thioester formation using standard Fmoc-chemistry. *Biopolymers* **71,** 352–353

21. Shogren-Knaak, M. A., and Peterson, C. L. (2004) Creating designer histones by native chemical ligation. *Methods Enzymol.* **375,** 62–76

22. Franz, H., Mosch, K., Soeroes, S., Urlaub, H., and Fischle, W. (2009) Multimerization and H3K9me3 binding are required for CDYL1b heterochromatin association. *J. Biol. Chem.* **284,** 35049–35059

23. Luger, K., Rechsteiner, T. J., and Richmond, T. J. (1999) Preparation of nucleosome core particle from recombinant histones. *Methods Enzymol.* **304,** 3–19

24. Huynh, V. A., Robinson, P. J., and Rhodes, D. (2005) A method for the in vitro reconstitution of a defined "30 nm" chromatin fibre containing stoichiometric amounts of the linker histone. *J. Mol. Biol.* **345,** 957–968

25. Schulze, W. X., and Mann, M. (2004) A novel proteomic screen for peptide-protein interactions. *J. Biol. Chem.* **279,** 10756–10764

26. Shevchenko, A., Tomas, H., Havlis, J., Olsen, J. V., and Mann, M. (2006) In-gel digestion for mass spectrometric characterization of proteins and proteomes. *Nat. Protoc.* **1,** 2856–2860

27. Cox, J., and Mann, M. (2008) MaxQuant enables high peptide identification rates, individualized p.p.b.-range mass accuracies and proteome-wide protein quantification. *Nat. Biotechnol.* **26,** 1367–1372

28. Huang da, W., Sherman, B. T., and Lempicki, R. A. (2009) Systematic and integrative analysis of large gene lists using DAVID bioinformatics resources. *Nat. Protoc.* **4,** 44–57

29. Vermeulen, M., Mulder, K. W., Denissov, S., Pijnappel, W. W., van Schaik, F. M., Varier, R. A., Baltissen, M. P., Stunnenberg, H. G., Mann, M., and Timmers, H. T. (2007) Selective anchoring of TFIID to nucleosomes by trimethylation of histone H3 lysine 4. *Cell* **131,** 58–69

30. Feng, W., Yonezawa, M., Ye, J., Jenuwein, T., and Grummt, I. (2010) PHF8 activates transcription of rRNA genes through H3K4me3 binding and H3K9me1/2 demethylation. *Nat Struct. Mol. Biol.* **17,** 445–450

31. Flanagan, J. F., Mi, L. Z., Chruszcz, M., Cymborowski, M., Clines, K. L., Kim, Y., Minor, W., Rastinejad, F., and Khorasanizadeh, S. (2005) Double chromodomains cooperate to recognize the methylated histone H3 tail. *Nature* **438,** 1181–1185

32. Shi, X., Hong, T., Walter, K. L., Ewalt, M., Michishita, E., Hung, T., Carney, D., Peña, P., Lan, F., Kaadige, M. R., Lacoste, N., Cayrou, C., Davrazou, F., Saha, A., Cairns, B. R., Ayer, D. E., Kutateladze, T. G., Shi, Y., Côté, J., Chua, K. F., and Gozani, O. (2006) ING2 PHD domain links histone H3 lysine 4 methylation to active gene repression. *Nature* **442,** 96–99

33. Wysocka, J., Swigut, T., Milne, T. A., Dou, Y., Zhang, X., Burlingame, A. L., Roeder, R. G., Brivanlou, A. H., and Allis, C. D. (2005) WDR5 associates with histone H3 methylated at K4 and is essential for H3 K4 methylation and vertebrate development. *Cell* **121,** 859–872

34. Lachner, M., O'Carroll, D., Rea, S., Mechtler, K., and Jenuwein, T. (2001) Methylation of histone H3 lysine 9 creates a binding site for HP1 proteins. *Nature* **410,** 116–120

35. Karagianni, P., Amazit, L., Qin, J., and Wong, J. (2008) ICBP90, a novel methyl K9 H3 binding protein linking protein ubiquitination with heterochromatin formation. *Mol. Cell Biol.* **28,** 705–717

36. Fischle, W., Franz, H., Jacobs, S. A., Allis, C. D., and Khorasanizadeh, S. (2008) Specificity of the chromodomain Y chromosome family of chromodomains for lysine-methylated ARK(S/T) motifs. *J. Biol. Chem.* **283,** 19626–19635

37. Kokura, K., Sun, L., Bedford, M. T., and Fang, J. (2010) Methyl-H3K9-binding protein MPP8 mediates E-cadherin gene silencing and promotes tumour cell motility and invasion. *EMBO J.* **29,** 3673–3687

38. Nozawa, R. S., Nagao, K., Masuda, H. T., Iwasaki, O., Hirota, T., Nozaki, N., Kimura, H., and Obuse, C. (2010) Human POGZ modulates dissociation of HP1alpha from mitotic chromosome arms through Aurora B activation. *Nat. Cell Biol.* **12,** 719–727

39. Cox, J., Matic, I., Hilger, M., Nagaraj, N., Selbach, M., Olsen, J. V., and Mann, M. (2009) A practical guide to the MaxQuant computational platform for SILAC-based quantitative proteomics. *Nat. Protoc.* **4,** 698–705

40. Zhang, K. M., Wang, Y. F., Huo, R., Bi, Y., Lin, M., Sha, J. H., and Zhou, Z. M. (2008) Characterization of Spindlin1 isoform2 in mouse testis. *Asian J. Androl* **10,** 741–748

41. D'Andrea, A. D. (2010) Susceptibility pathways in Fanconi's anemia and breast cancer. *N. Engl. J. Med.* **362,** 1909–1919

42. Mandel, S., Rechavi, G., and Gozes, I. (2007) Activity-dependent neuroprotective protein (ADNP) differentially interacts with chromatin to regulate genes essential for embryogenesis. *Dev. Biol.* **303,** 814–824

43. Beever, C., Lai, B. P., Baldry, S. E., Peñaherrera, M. S., Jiang, R., Robinson, W. P., and Brown, C. J. (2003) Methylation of ZNF261 as an assay for determining X chromosome inactivation patterns. *Am. J. Med. Genet. A* **120A,** 439–441

44. Smothers, J. F., and Henikoff, S. (2000) The HP1 chromo shadow domain binds a consensus peptide pentamer. *Curr. Biol.* **10,** 27–30

45. Déjardin, J., and Kingston, R. E. (2009) Purification of proteins associated with specific genomic Loci. *Cell* **136,** 175–186

46. Bartke, T., Vermeulen, M., Xhemalce, B., Robson, S. C., Mann, M., and Kouzarides, T. (2010) Nucleosome-interacting proteins regulated by DNA and histone methylation. *Cell* **143,** 470–484

47. Bonasio, R., Lecona, E., and Reinberg, D. (2010) MBT domain proteins in development and disease. *Semin Cell Dev. Biol.* **21,** 221–230

48. Bernstein, B. E., Mikkelsen, T. S., Xie, X., Kamal, M., Huebert, D. J., Cuff, J., Fry, B., Meissner, A., Wernig, M., Plath, K., Jaenisch, R., Wagschal, A., Feil, R., Schreiber, S. L., and Lander, E. S. (2006) A bivalent chromatin structure marks key developmental genes in embryonic stem cells. *Cell* **125,** 315–326

49. Allis, C. D., Jenuwein, T., Reinberg, D. (eds.), Caparros, M. L. (assoc. ed.) (2006) Epigenetics, Cold Spring Harbor Laboratory, Cold Spring Harbor, NY

50. Luger, K., Mäder, A. W., Richmond, R. K., Sargent, D. F., and Richmond, T. J. (1997) Crystal structure of the nucleosome core particle at 2.8 A resolution. *Nature* **389,** 251–260

51. Woodcock, C. L., and Ghosh, R. P. (2010) Chromatin higher-order structure and dynamics. *Cold Spring Harb Perspect Biol.* **2,** a000596

52. Shogren-Knaak, M., Ishii, H., Sun, J. M., Pazin, M. J., Davie, J. R., and Peterson, C. L. (2006) Histone H4-K16 acetylation controls chromatin structure and protein interactions. *Science* **311,** 844–847

53. Thiru, A., Nietlispach, D., Mott, H. R., Okuwaki, M., Lyon, D., Nielsen, P. R., Hirshberg, M., Verreault, A., Murzina, N. V., and Laue, E. D. (2004) Structural basis of HP1/PXVXL motif peptide interactions and HP1 localisation to heterochromatin. *EMBO J.* **23,** 489–499

54. Jensen, L. J., Kuhn, M., Stark, M., Chaffron, S., Creevey, C., Muller, J., Doerks, T., Julien, P., Roth, A., Simonovic, M., Bork, P., and von Mering, C. (2009) STRING 8-a global view on proteins and their functional interactions in 630 organisms. *Nucleic Acids Res.* **37,** D412–416

55. Rosenfeld, J. A., Wang, Z., Schones, D. E., Zhao, K., DeSalle, R., and Zhang, M. Q. (2009) Determination of enriched histone modifications in non-genic portions of the human genome. *BMC Genomics* **10,** 143

56. Cochrane, G. R., and Galperin, M. Y. (2010) The 2010 Nucleic Acids Research Database Issue and online Database Collection: a community of data resources. *Nucleic Acids Res.* **38,** D1–4

57. Sims, R. J., 3rd, Chen, C. F., Santos-Rosa, H., Kouzarides, T., Patel, S. S., and Reinberg, D. (2005) Human but not yeast CHD1 binds directly and selectively to histone H3 methylated at lysine 4 via its tandem chromodomains. *J. Biol. Chem.* **280,** 41789–41792

58. Bannister, A. J., Zegerman, P., Partridge, J. F., Miska, E. A., Thomas, J. O., Allshire, R. C., and Kouzarides, T. (2001) Selective recognition of methylated lysine 9 on histone H3 by the HP1 chromo domain. *Nature* **410,** 120–124